JOURNAL OF APPLIED ELECTROCHEMISTRY 17 (1987) 1002–1020

State of overpotential-deposited H species at electroplated platinum surfaces in comparison with bright platinum

MEIR ELAM, B. E. CONWAY

Chemistry Department, University of Ottawa, 365 Nicholas Street, Ottawa, Canada K1N 9B4

Received 30 June 1986; revised 2 January 1987

The state of chemisorbed H at platinum electrodes, having a large roughness factor (high real-to-apparent area ratio), is of interest in relation to operation of the reversible H_2 electrode and to the performance of water electrolyser cathodes and fuel cell anodes.

Results are reported of investigations of the behaviour of overpotential-deposited (OPD) H at high-area platinum surfaces generated by electroplating platinum, with and without lead as an additive, on a platinum substrate in the form of a rotating disc electrode. Comparisons are made with the behaviour of OPD H at an anodically activated, bright platinum electrode surface. The sorption behaviour of the OPD H is evaluated from digitally acquired open-circuit potential-decay transients which enable the potential dependence of OPD H coverage (the H pseudocapacitance) and the change of H coverage over a range of H_2 evolution current densities to be derived. Use of rotated platinum electrodes (4900 r.p.m.) enables possible interference from effects of H_2 supersaturation in solution to be avoided or minimized.

At active platinum surfaces, the apparent extent of OPD H sorption substantially exceeds a monolayer, depending on the electroplating procedure, with or without lead as additive, or at the bright platinum surface in acid solution. The OPD H coverage is related to the activity of platinum surfaces as H_2 evolution electrocatalysts.

At electroplated palladium, where H sorption is well known, the potential decay behaviour is similar to that at platinum in acid, thus supporting the role of H sorption in the near-surface region at the latter metal.

1. Introduction

Relatively detailed information is now available on the thermodynamic [1] and kinetic [1, 2] behaviour of underpotential-deposited (UPD) H at platinum and other noble metals. In contrast, rather little quantitative information exists on the coverage and potential dependence of coverage of the adsorbed H, that is the kinetically involved intermediate species in the cathodic hydrogen evolution reaction (HER) at appreciable current densities and corresponding overpotentials. We have referred to this H as the 'overpotential-deposited' (OPD) H in the HER.

The state of chemisorbed H at platinum cathodes is of much interest in relation to the mechanisms of the HER at this metal under various conditions, and in relation to practical aspects of the performance of platinum electrodes as fuel cell anodes and water electrolyser or electrochemical hydrogenator cathodes.

A recent paper [4] has reviewed earlier work on this question, based on a.c. impedance [5] and charging curve evaluation [6] at platinum, and has presented new results on the determination of the OPD H coverage in the HER, and its potential dependence, at nickel, nickel–molybdenum alloy electrodes [3], gold and smooth active platinum electrodes [4]. These results allowed a rationalization to be made of the conditions required for low Tafel slopes (b) for the HER to arise at these electrode

0021–891X/87 $03.00 + .12

materials in terms of experimentally determined potential dependence of OPD H coverage, together with the charge transfer symmetry factor β ($\simeq 0.5$). Not only highest possible values of the exchange current density, i_0, but low values of b are required for optimum performance of water electrolyser cathodes and anodes at practically high operating current densities, $\geqslant 10^{-1}\,\mathrm{A\,cm^{-2}}$.

High-area platinum electrocatalyst materials are prepared by chemical-, or electrodeposition onto carbon substrates or by electroplating onto metal substrates [7]. In the present paper, we report studies on the state of OPD H in the HER on two kinds of high-area platinum surfaces formed by electroplating, with and without lead as additive, in relation to the behaviour at anodically activated bright platinum. The possible role of a state of sorbed, as well as adsorbed, H is indicated (a surface-region hydride phase) in the HER at platinum surfaces in acid solution. By comparative measurements on the HER and the behaviour of its OPD H at a palladium electrode, where H sorption is well established, the apparent sorption behaviour of OPD H at platinum is clarified.

The methods employed in this work are: (i) steady-state evaluation of the log of current density, i, versus overpotential, η relations by means of a computer-controlled potential programme coupled with (ii) digital acquisition and computer processing of potential relaxation transients, following interruption of the polarizing currents at various corresponding overpotentials.

2. Experimental details

2.1. *Solutions*

Aqueous KOH solutions (1 M) were prepared by double recrystallization of AnalaR KOH in a N_2 atmosphere from pyrodistilled water [8] and dissolved in the requisite volume of such water. In some experiments the solutions were pre-electrolysed.

2.2. *Cell and electrodes*

A conventional three-compartment, all-glass cell was used. Purified H_2 gas saturated with vapour from pyrodistilled water was bubbled continuously through the compartments.

The working electrode was a platinum rotating disc mounted in Teflon (Pine Instrument Co.) and had a geometric area of $0.5\,\mathrm{cm^2}$. The electrode was polished employing a fine alumina powder ($0.05\,\mu$m particle size) and washed with distilled water in an ultrasonic cleaner. Two platinization methods were employed, both using 2% chloroplatinic acid. One utilized 0.02% lead acetate [7] and the other employed no lead additive [9]. The various kinds of platinum electrodes (including the smooth, bright one) all underwent a preliminary electrochemical pretreatment [10] in sulphuric acid prior to introduction into the working solution. This consisted of pulsed polarization to $+1.8\,\mathrm{V}\,E_{H_2}$ for 10 s followed by polarization to 1.2 V for 30 s and reduction at $+0.05$ V for 30 s, repeated five times.

It was found that above 3000 r.p.m. the i versus η relations were reproducible and independent of further increase of electrode rotation rate. All i versus η and potential decay measurements were performed at 4900 r.p.m.

The real surface area was calculated from the charges under the hydrogen UPD peaks [11] determined by cyclic voltammetry in 0.5 M H_2SO_4 and/or 1 M KOH. The surface area was also determined from double-layer capacity measurement. This capacitance was estimated from the first 10 to 20 μs of potential decay [12], just after the jump in potential due to iR drop. The surface area thus calculated was within 30% of the results obtained by the cyclic voltammetry method, taking the double-layer capacitance per real $\mathrm{cm^2}$ of platinum surface as $20\,\mu\mathrm{F\,cm^{-2}}$ over the potential range for UPD H accommodation at platinum.

The reference electrode used was a reversible hydrogen electrode at platinum in the same solution. The iR drop between the Luggin capillary of the reference electrode and the working electrode was

determined at various current densities by the current interruption procedure, using a Nicolet digital oscilloscope. The solution resistance was evaluated from the potential difference between the overall potential and the overpotential at $t = 0$, obtained by extrapolation over the first 5–20 μs. A plot of this potential difference versus the initial polarization current (at least 10 points) gave a straight line that passed through the origin, with an excellent correlation coefficient (more than 0.999). The solution resistance is the slope of this line. The resistances involved were about $2.0 \pm 0.1\,\Omega$, depending on geometry. The solution resistance determined with an accuracy of 1–2% was confirmed, in some cases, by means of a.c. impedance using a Solartron frequency analyser. Owing to the high currents (up to 0.7 A) which pass at the rotating disc electrode, the equivalent reaction resistance may be as low as 10–20% of the solution resistance in series with it, so that accurate measurement of the latter becomes of major importance.

The counter electrode consisted of a platinum gauze mounted on a platinum wire sealed into soft glass tubing.

2.3. *Electrical measurements*

The polarization measurements were performed by means of Wenking HP72 potentiostat controlled by a Hewlett-Packard 87 microcomputer through a Kepco SN 488-122 Programmer (D/A converter) and Keithley Model 195 DMM (A/D converter). The software developed allows application of a staircase waveform or a progressive square-wave pulse sequence waveform. The latter was extensively used and enabled a highly reproducible polarization curve to be obtained. The base potential was programmed to some anodic activation potential, say +1.0 V, and after a predetermined time, it was jumped to the required cathodic value for another predetermined time, usually 8–10 s, and then the current was measured and its value stored in the computer memory. This cycle was continued until the final required cathodic potential was reached.

All the data were recorded on a floppy disc for further analysis and replotting. It was found that activation times above 2 s did not usually significantly improve the exchange current density values and their reproducibility. However, a standardized time of 8 s was used for all the experiments that gave the results recorded here, in order to ensure the best conditions. The same activation process was employed prior to each potential decay measurement (see below).

Potential decay transients were initiated from various cathodic overpotentials by interruption of the corresponding polarizing current by means of a Clare vacuum Hg relay switch triggered by a debounced micro-switch. The resulting potential versus time relaxation transients were digitally recorded by means of a Nicolet 3091 digital oscilloscope and stored on a floppy disc. The method for processing the open-circuit potential relaxation data was as reported recently [3, 13] and the basis and requirements of the computational procedure used was fully described in those publications, while theoretical aspects of the interpretation of the results have been published elsewhere [14].

The digitally acquired $\eta(t)$ data were processed in the microcomputer to derive the adsorption pseudo-capacitance associated with the dependence of the OPD H coverage on the HER overpotential, η, after computing $\mathrm{d}\eta/\mathrm{d}t$.

All measurements were performed at 296 ± 1 K.

2.4. *Processing of the experimental data*

While the data processing procedure and theoretical aspects of the treatment of potential decay transients required to obtain the results reported below were recorded in our earlier papers [3, 13–15], it will be convenient briefly to summarize the operations employed.

Potential decay transients, $\eta(t)$, are recorded digitally from various η values corresponding to current interruption from polarizing current densities, i. Under the same experimental conditions, η as $f(\ln i)$, the Tafel relation, is determined by means of a computer-controlled potentiostatic system.

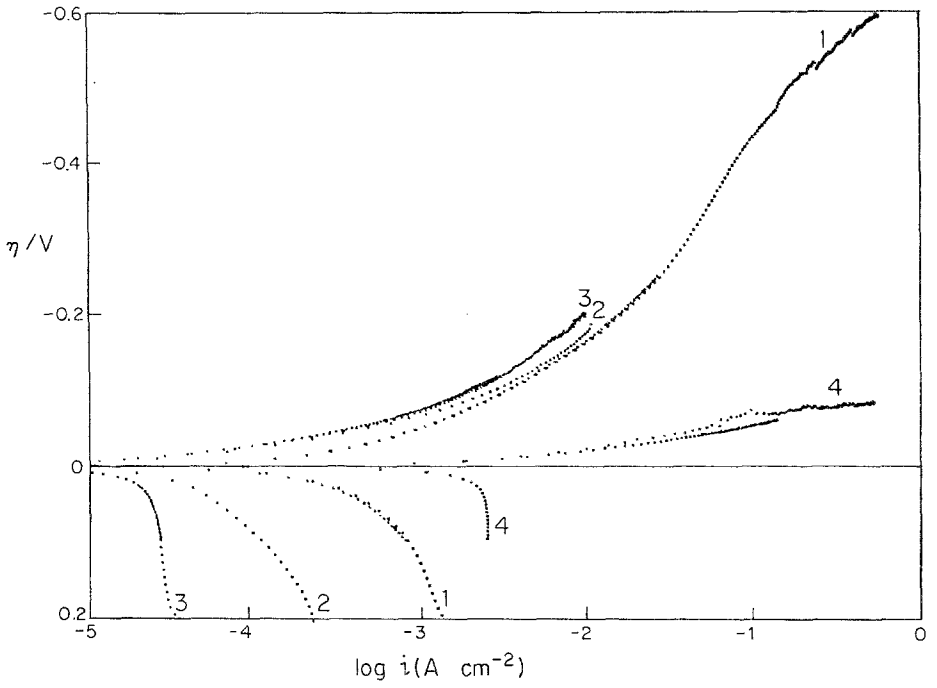

Fig. 1. Tafel plots for HER on disc electrodes at a rotation rate of 4900 r.p.m. (1) Bright platinum, roughness factor (RF) = 1.8, 1 M KOH (two runs). (2) Unleaded electrodeposited platinum, RF = 20, 1 M KOH. (3) Leaded electrodeposited platinum, RF = 100, 1 M KOH (two runs). (4) Bright platinum, RF = 1.6, 0.5 M H_2SO_4.

The interfacial capacitance, $C(\eta)$, which is normally a f(η), is

$$-C(\eta)\,\mathrm{d}\eta/\mathrm{d}t = i_0 \exp(\alpha\eta F/RT)$$

which determines the behaviour of the potential decay. This potential-decay rate equation can be integrated [13, 16] to give η as the f ln($t + \tau$) in time, t, plus an integration constant, τ [16], with a characteristic slope $\mathrm{d}\eta/\mathrm{d}\ln(t + \tau)$ that is determined jointly by the Tafel slope, $b = RT/\alpha F$, and by any potential-dependence of C.

As we have shown elsewhere [3, 4, 13], it is useful to process the $\eta(t)$ data in three ways:

(i) as plots [15, 16] of $\eta(t)$ as f(ln t) or ln($t + \tau$);

(ii) as plots [13] of $\eta(t)$ versus ln($-\mathrm{d}\eta/\mathrm{d}t$) which should have slopes having the same numerical value as $\mathrm{d}\eta/\mathrm{d}\ln(t + \tau)$; and

(iii) by evaluation of $C(\eta)$ as f(η) from $-i_0[\exp(\alpha\eta F/RT)]/\mathrm{d}\eta/\mathrm{d}t$.

The latter dependence of $C(\eta)$ on η gives, to a good approximation, the potential dependence of the pseudocapacitance, $C_\phi(\eta)$, associated with potential-dependence of coverage by the adsorbed electroactive intermediate in the reaction [14, 17], H in the present case, for conditions where $C_\phi \gg C_{\mathrm{dl}}$, the double-layer capacitance. A principal aim of the work is the evaluation of $C(\eta)$ for the electroactive adsorbed species. The additive (or otherwise) relation between $C_\phi(\eta)$ and C_{dl} has been discussed in other papers [4, 14], in relation to the equivalent circuit.

3. Results

3.1. *Log (current density) versus potential relationships*

Tafel plots for various platinum electrodes in 1 M KOH solution are shown in Fig. 1. The plot in acidic solution for a bright platinum electrode is given for comparison.

The roughness factor of the electrodes is reflected in the kinetic behaviour on the anodic polarization (hydrogen oxidation) side. The limiting current *densities* differ according to the real area because the H_2 oxidation is mass-transfer controlled and thus depends merely on the geometrical area. However, the absolute limiting currents are almost the same for all the electrodes as the geometrical areas were virtually the same.

On the cathodic (hydrogen evolution) side, for the alkaline solutions, the curves are quite close to each other, considering the different electrodes involved. The reproducibility within each system is excellent.

The cathodic Tafel slope at low overpotentials (calculated after correction for the back-reaction current component) is -0.037 V per decade for the electroplated electrodes and -0.064 V per decade for the bright electrode. Beyond $\eta = \sim -0.05$ V the plot for bright platinum exhibits a continuously increasing curvature, reaching a nominal slope of ~ -0.37 V per decade at -0.3 to -0.4 V. At $\eta = \sim -0.4$ V there is an inflection in the curvature, the slope changing to the nominal value of -0.18 V per decade in the overpotential range of -0.5 to -0.6 V. This behaviour implies a variable reaction mechanism at bright platinum, with a parallel reaction pathway [3], as will be discussed below.

3.2. *Potential decay behaviour*

Two sets of the digitally acquired potential relaxation data for a bright platinum electrode in 1 M KOH are shown in Fig. 2. The corresponding η versus log $(-\mathrm{d}\eta/\mathrm{d}t)$ plots are given in Fig. 3 (for the sake of clarity, only one out of two curves is shown). These potential decay curves exhibit an interesting dependence on the initial polarization current densities which cover a wide range of almost three decades of current (0.0011–0.78 A cm^{-2}).

Fig. 2a and the corresponding Fig. 3a is similar to those described in previous work [4]. Note, however, that the five curves depicted in ref. 4 of Fig. 5 correspond approximately to curves 6 to 8 in Fig. 2a. As discussed previously [14], η is strictly only a linear function in $\ln(t + \tau)$ as $C_\phi = 0$ or constant [15, 16]. Therefore, when $t < \tau$, the relation between η and $\ln(t)$ will depend on the initial current, i_{in} $(\tau = bC_{dl}/i_{in})$ as seen in Fig. 2a. However, in η versus log $(-\mathrm{d}\eta/\mathrm{d}t)$ plots, processed according to the equation

$$-\mathrm{d}\eta/\mathrm{d}t = \mathrm{i}(\eta)/(C_{dl} + C_\phi)$$

a dependence of the resulting behaviour on the initial current is avoided. In Fig. 3a, at the higher i_{in}, the curves almost coincide, exhibiting two principal decay regions as was pointed out previously [4]. As the initial current decreases, one of these regions disappears corresponding to the decreasing curvature of the Tafel plots (Fig. 1).

An interesting phenomenon arises when i_{in} is above 0.08 A cm^{-2}, as shown in Figs 2b and 3b. Up to $t = \sim 10$ ms, the decay is faster as i_{in} increases, i.e. at a given time the relaxation potential is lower as the i_{in} is higher. At times longer than 10 ms, the curves coincide. This corresponds to the inflection of the Tafel slope (Fig. 1, curve 1). Above 0.08 A cm^{-2} $(\eta = \sim -0.4$ V) the slope diminishes, indicating that the faradaic reaction resistance becomes lower.

For comparison, corresponding plots for a bright platinum electrode in 0.5 M H_2SO_4 are also given (Fig. 4). Although the i_{in} for the acidic and alkaline solutions are in a similar range, the above phenomenon does not arise in the acidic solution as the overpotential range is different.

The potential decay curves and the log $(-\mathrm{d}\eta/\mathrm{d}t)$ plots for leaded and unleaded electrodeposited platinum in 1 M KOH are given in Figs 5 to 8, respectively (For the sake of clarity, only one out of two experimental curves is shown in Fig. 6.). Figs 5 and 7 are similar to Fig. 2a in that, at a given time, the relaxation potential is lower as the i_{in} is lower, but the general shapes of the curves are similar to those depicted in Fig. 2b. Note the difference in the i_{in} range between the data for the electrodeposited electrodes and the bright one. At the latter, much higher initial polarization current densities were attained.

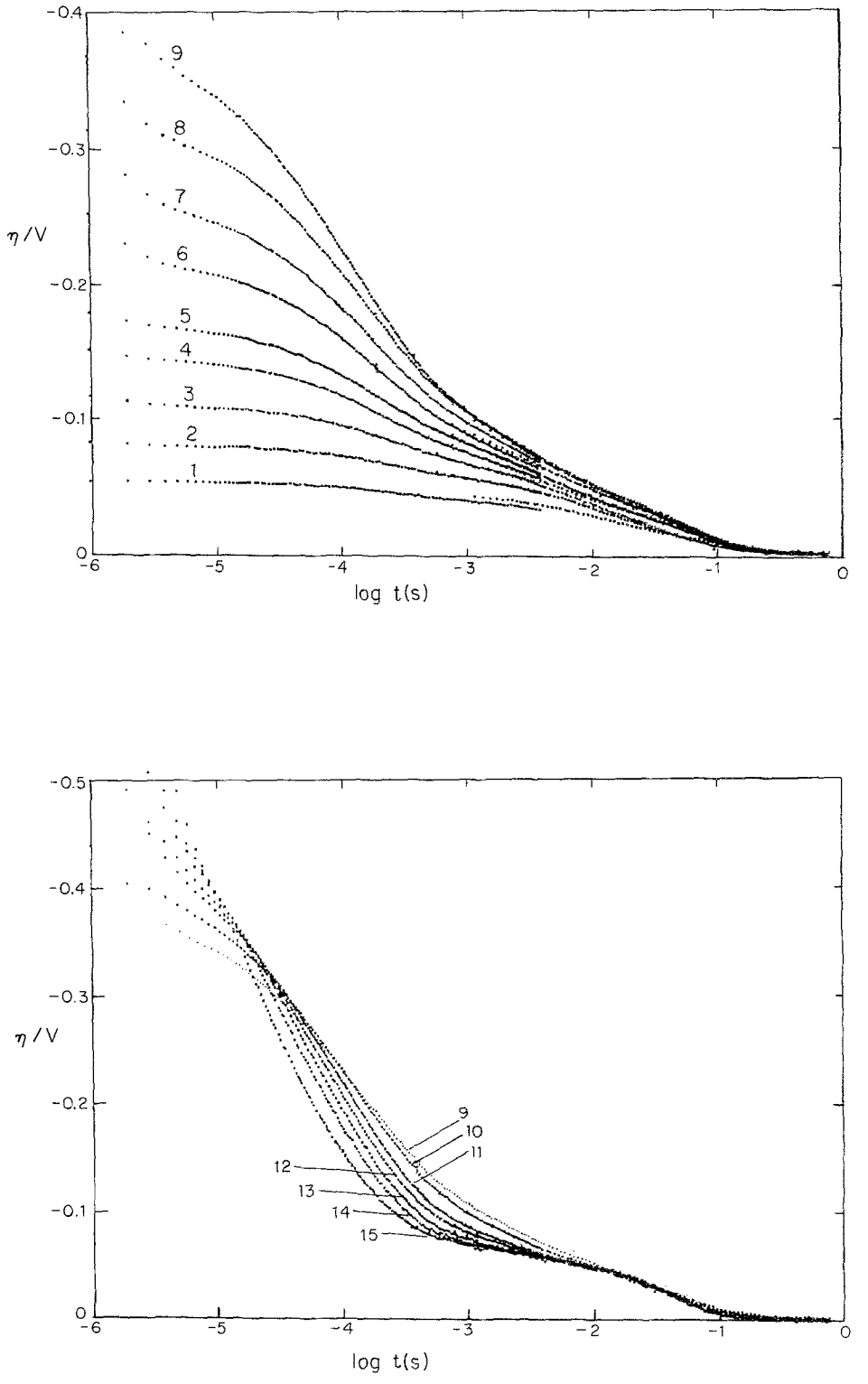

Fig. 2. Potential decay plots for the HER at a rotation rate of 4900 r.p.m. for a bright platinum electrode in 1 M KOH. The initial polarization currents in A cm^{-2} are: (1) 0.0011; (2) 0.0022; (3) 0.0044; (4) 0.0089; (5) 0.0133; (6) 0.022; (7) 0.033; (8) 0.050; (9) 0.078; (10) 0.111; (11) 0.167; (12) 0.22; (13) 0.33; (14) 0.50; (15) 0.78.

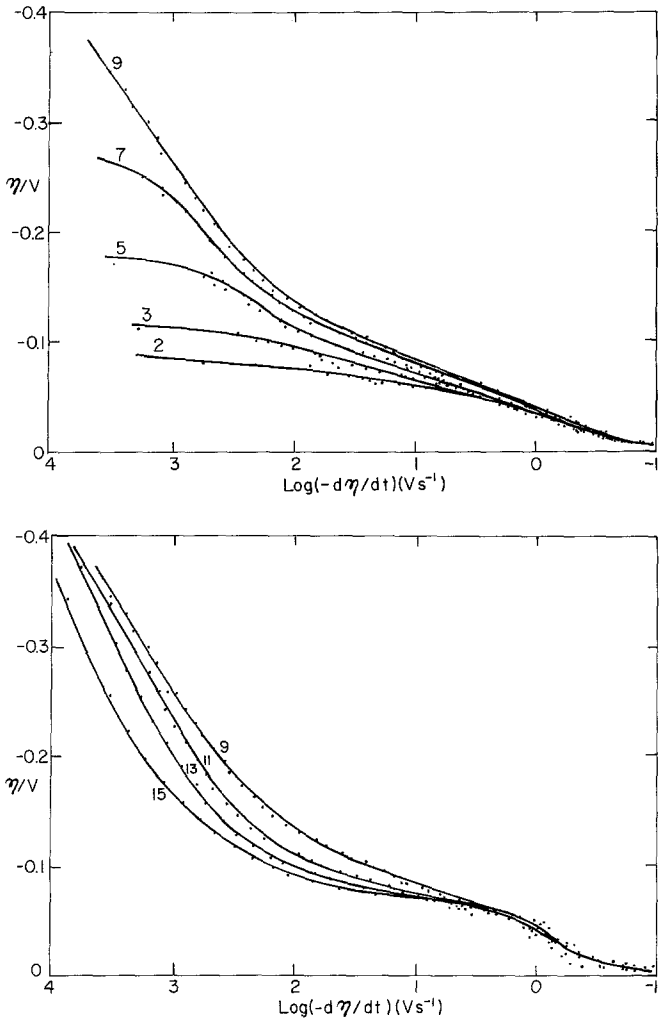

Fig. 3. Plots of η versus log $(-\mathrm{d}\eta/\mathrm{d}t)$ for the data shown in Fig. 2.

Attention is directed to the remarkable difference between the various electrodes with respect to the total time lapse required for the potential decay processes to be effectively completed (i.e. for the potential to decay, say, to within 2 mV of the reversible potential). Although it takes less than 0.2 s for the bright electrodes, it takes about 7–8 s for the electrodeposited (leaded) one or even more than 60 s for the unleaded one*.

If the only difference between the electrodes was the surface area, this time lapse should be the same for all the electrodes. This observation probably indicates that different states of adsorption of H species are involved in each of the cases, perhaps depending on orientation of micro-crystal faces. For example, two arrest regions can be distinguished in Figs 5 and 7 for the plated platinum surfaces that are not observed at bright platinum.

The slopes of the η versus log $(-\mathrm{d}\eta/\mathrm{d}t)$ plots below $\eta = -0.1$ V are 29 mV per decade for the unleaded electroplated electrode, 33 mV per decade for the leaded electroplated electrode, and vary from 36 mV per decade at the lowest i_{in} applied to 66 mV per decade at the highest i_{in} for the bright

* The possibility is recognized that the difference between bright and platinized platinum electrodes might originate from H arising from supersaturated H_2 in the solution boundary layer [6]. However, the point of conducting the experiments at rotated electrodes was to eliminate (or minimize) such effects (cf. [4]). Also, under the rotation conditions used, such effects could hardly be expected to persist on open circuit into the 10^0 to 10^2 decades (Figs 5, 7) of time range under rotation at $\geqslant 3600$ r.p.m.

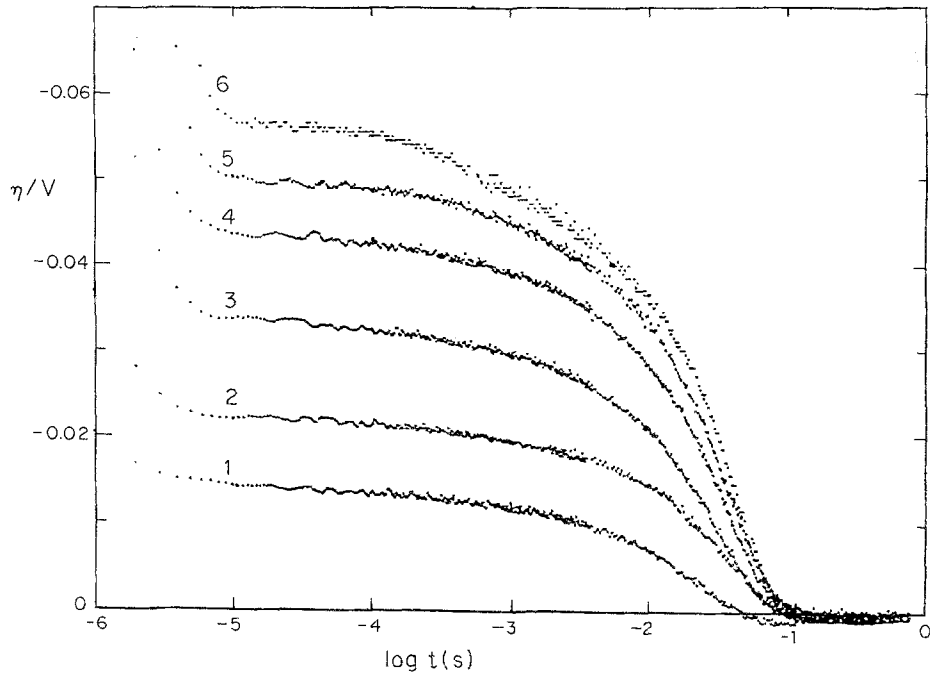

Fig. 4. Plots as Fig. 2 but for 0.5 M H_2SO_4. The initial polarization currents in A cm^{-2}: (1) 0.063; (2) 0.013; (3) 0.038; (4) 0.088; (5) 0.188; (6) 0.56.

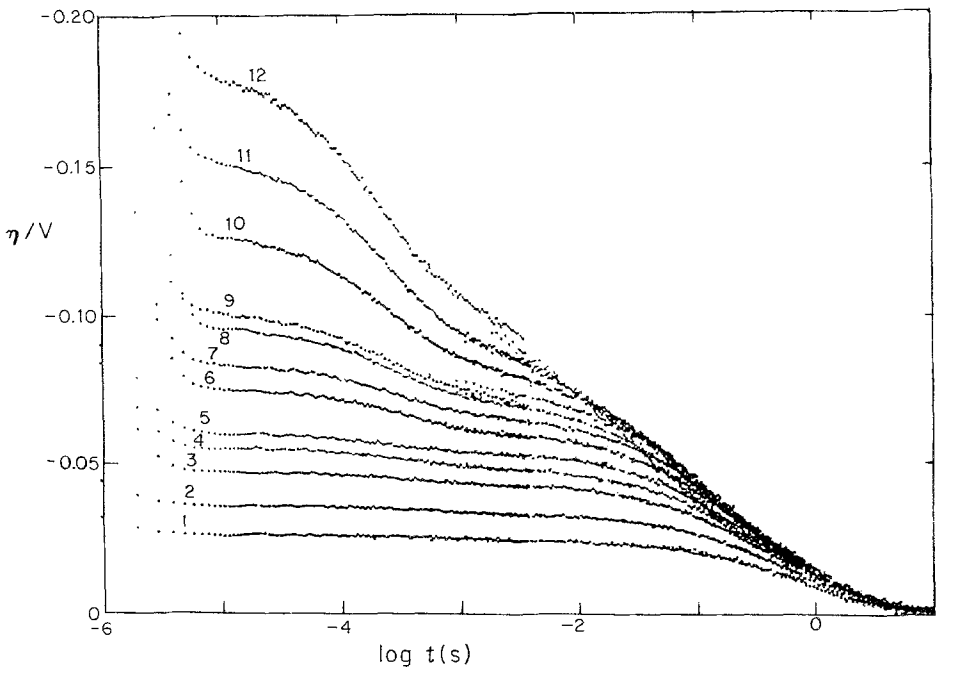

Fig. 5. Plots as for Fig. 2 but for leaded electrodeposited platinum electrode. The initial polarization currents in A cm^{-2} are: (1) 0.0001; (2) 0.0002; (3) 0.0004; (4) 0.0006; (5) 0.0009; (6) 0.0012; (7) 0.0020; (8) 0.0030; (9) 0.0040; (10) 0.0060; (11) 0.0090; (12) 0.014.

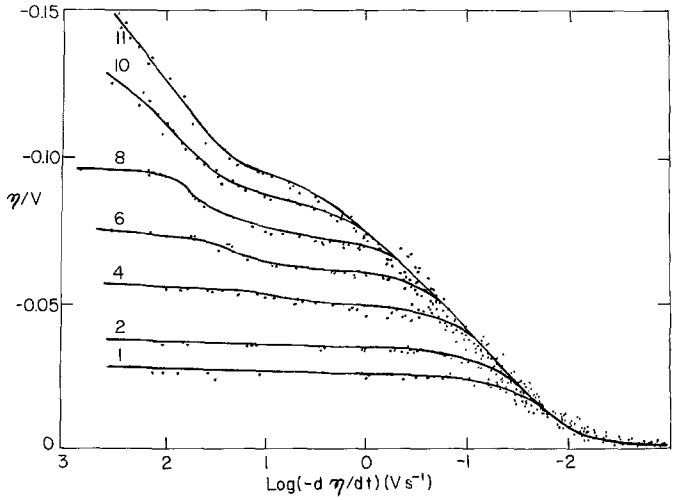

Fig. 6. Plots of η versus log $(-\mathrm{d}\eta/\mathrm{d}t)$ for the data given in Fig. 5.

electrode in 1 M KOH. For $\eta > 0.15$ V, the slope for the bright electrode increases with an increase of the i_{in}, exceeding 200 mV per decade for the highest i_{in} applied.

4. Discussion

4.1. *Current density versus potential relationships*

Two accepted [18, 19] paths for the HER in alkaline solutions are as follows. A primary discharge step:

$$\mathrm{M} + \mathrm{H_2O} + e \underset{k_{-1}}{\overset{k_1}{\rightleftharpoons}} \mathrm{MH_{ads}} + \mathrm{OH^-} \qquad \mathrm{I}$$

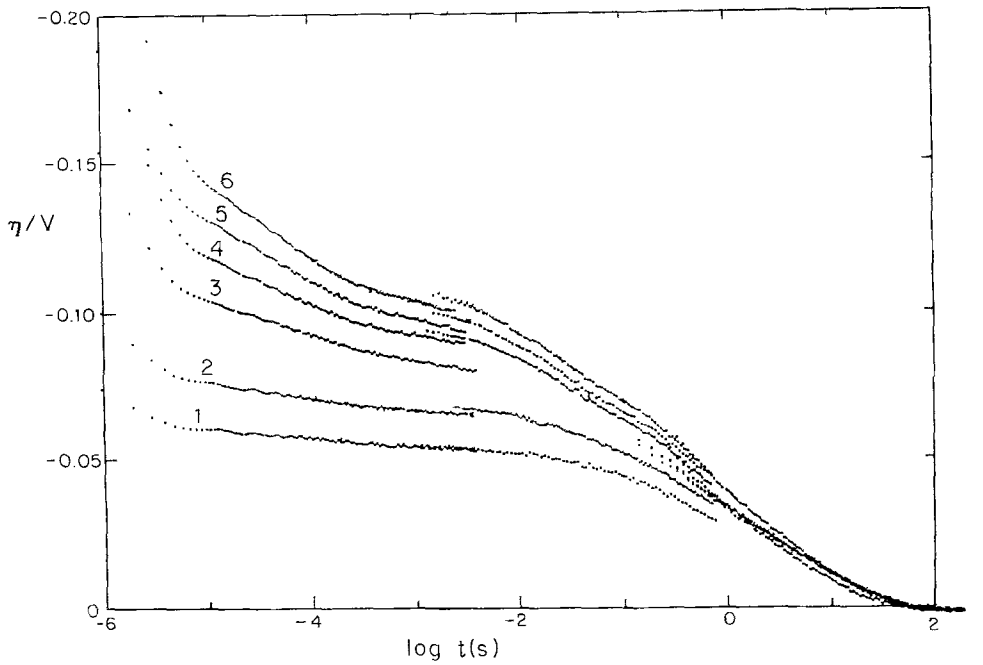

Fig. 7. Plots as Fig. 2 but for unleaded electrodeposited platinum electrode. The initial polarization currents in A cm^{-2} are: (1) 0.001; (2) 0.002; (3) 0.004; (4) 0.06; (5) 0.08; (6) 0.010.

coupled either with the electrochemical desorption step,

$$MH_{ads} + H_2O + e \underset{k_{-2}}{\overset{k_2}{\rightleftharpoons}} H_2 + OH^- + M \qquad \text{II}$$

or the H recombination desorption step,

$$MH_{ads} + MH_{ads} \underset{k_{-3}}{\overset{k_3}{\rightleftharpoons}} H_2 + 2M \qquad \text{III}$$

The fact that the OPD H coverage is still appreciable ($\theta = 0.3$ at $\eta = -0.09$ V, as will be shown later) indicates [20] that the rate constant of the electrochemical desorption step is not small in comparison to that of the initial discharge step, i.e. quasi-equilibrium in the latter is not maintained. Moreover, in alkaline solution, discharge is usually more difficult than in acid, so if k_3 remains independent of pH (apart from any anion adsorption effect), the rate constant of the primary discharge step I can become comparable to k_3 for the recombination step and, at lower overpotentials, the recombination pathway will be favoured. This kind of kinetic situation has been treated in previous publications [3, 4]. In the present treatment, the back reactions for steps II and III were also taken into account [21].

The relevant rate equations are:

$$v_1 = k_1(1 - \theta)\exp(\beta\eta f) = l(1 - \theta)$$

$$v_{-1} = k_{-1}\theta C_{OH}\exp[-(1 - \beta)\eta f] = m\theta \qquad (11)$$

$$v_2 = k_2\theta\exp(\gamma\eta f) = n\theta \qquad (12)$$

$$v_{-2} = k_{-2}(1 - \theta)C_{OH}\exp[-(1 - \gamma)\eta f] = h\theta \qquad (13)$$

$$v_3 = k_3\theta^2 \qquad (14)$$

$$v_{-3} = k_{-3}(1 - \theta)^2 \qquad (15)$$

where $f = F/RT$, β and γ are symmetry factors for charge transfer, and l, m, n and h are defined obviously according to Equations 10 to 13 and are functions of η.

The steady-state condition for H coverage is then

$$d\theta/dt = 0 = v_1 + v_{-2} + v_{-3} - v_{-1} - v_2 - v_3 \qquad (16)$$

Substituting Equations 10–15 into Equation 16 results in

$$(k_3 - k_{-3})\theta^2 + (1 + m + n + h + 2k_{-3})\theta - (l + h + k_{-3}) = 0 \qquad (17)$$

the solution of which is

$$\theta = \{[(l + m + n + h + 2k_{-3})^2 + 4(k_3 - k_{-3})(l + h + k_{-3})]^{1/2} - (l + m + n + h + 2k_{-3})\}/2(k_3 - k_{-3}) \qquad (18)$$

and the corresponding capacitance for OPD H ($q\,d\theta/d\eta$) is

$$C_\phi = qf/2(k_3 - k_{-3})\{[(l + m + n + h + 2k_{-3})^2 + 4(k_3 - k_{-3}) \times (l + h + k_{-3})]^{-1/2}[(l + m + n + h + 2k_{-3})(l - m + n - h) + 2(k_3 - k_{-3}) \times (l - h)] - (l + m + n - h)\} \qquad (19)$$

where q is the charge for deposition of a monolayer of H and taking $\beta = \gamma = 0.5$. The total current density can be expressed in the form

$$i/2F = v_1 - v_{-1} = (v_2 - v_{-2}) + (v_3 - v_{-3}) \qquad (20)$$

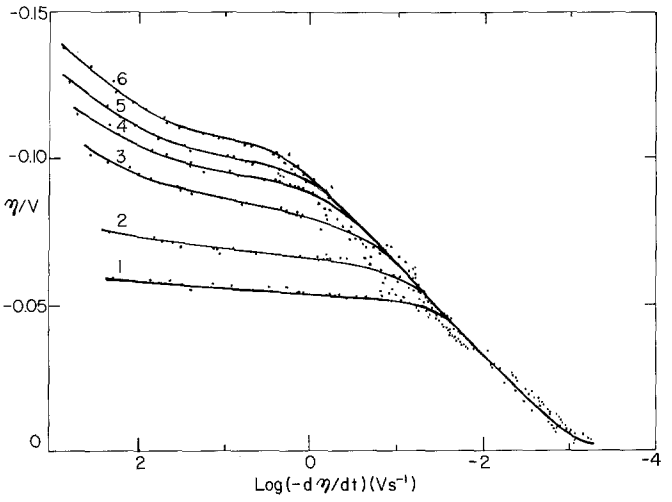

Fig. 8. Plots of η versus log $(-\mathrm{d}\eta/\mathrm{d}t)$ for the data given in Fig. 7.

and represents the situation that the recombination and the electrochemical desorption steps are involved as parallel paths. The contribution to the reaction rate of each of the parallel paths depends, of course, on the respective rate constants but, generally, the electrochemical desorption step always tends to becomes dominant at high overpotentials because v_2 increases exponentially with η whereas v_3 tends to a constant as θ tends to its saturation limiting value.

This situation is represented in Fig. 9 which is a simulated Tafel plot calculated for the parallel mechanism using Equation 20 combined with Equations 12–15 and 18. The corresponding C_ϕ versus η and θ versus η plots calculated from Equations 18 and 19, respectively, are shown in Fig. 10. It

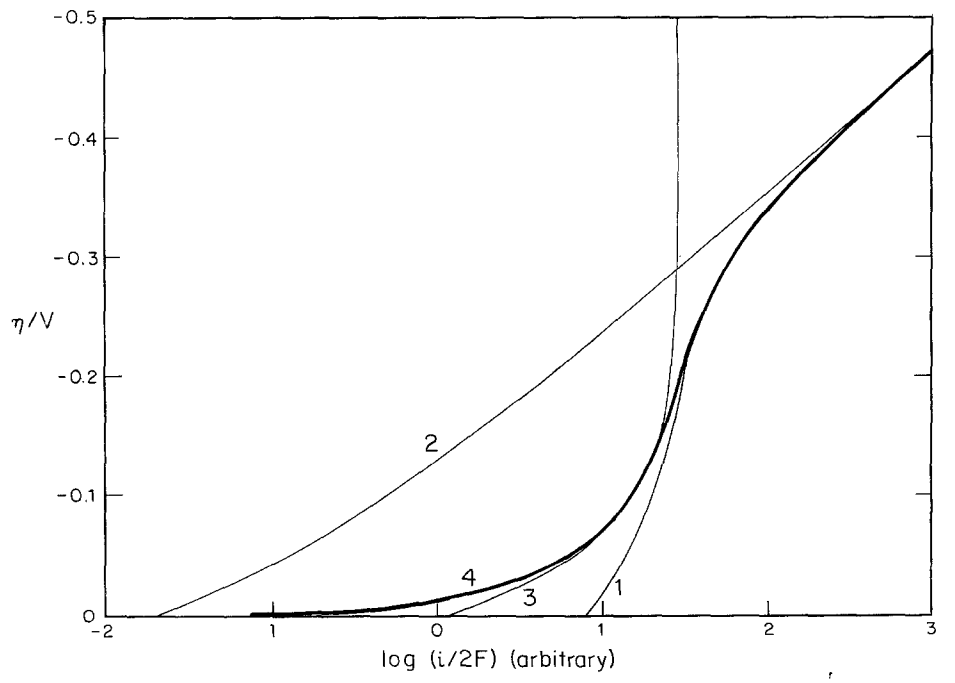

Fig. 9. Simulated Tafel plots using the following values of rate constants: $k_1 = 10$; $k_{-1} = 40$; $k_2 = 0.1$; $k_{-2} = 0.05$; $k_3 = 30$; $k_{-3} = 2$. (1) Reaction I (Equation 10); (2) Reaction II (Equation 12); (3) Reaction III (Equation 14); (4) The total reaction rate according to Equation 20.

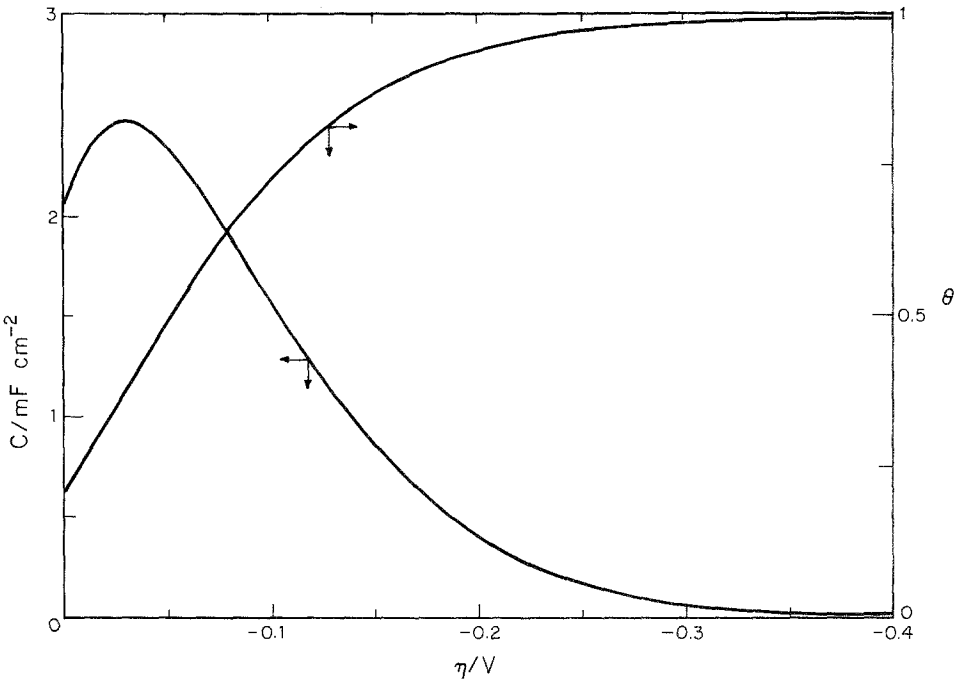

Fig. 10. Calculated coverage and pseudocapacitance plots according to Equations 18 and 19. The values of the rate constants taken as in Fig. 9.

is seen that the form of the Tafel plot thus calculated (Fig. 9, curve 4) is very similar to the form of the experimental Tafel plot (Fig. 1, curve 1).

Curves 1 to 3 in Fig. 9 represent the partial forward current contributions to the total resulting current (curve 4). (The partial backward reaction currents are not drawn in Fig. 9 for the sake of clarity, although their contributions are important at low overpotentials.) It is seen that up to $\eta = \sim -0.2\,\text{V}$ the recombination pathway makes the dominant contribution to the total rate associated with the parallel desorption steps. The ratio k_3/k_2 is 300 in this example and the exponential growth in v_2 is accompanied by a rapid increase in θ ($v_3 \propto \theta^2$) in this range of overpotentials (cf. Fig. 10). Beyond this overpotential, v_3 tends to a constant value as θ tends to its limiting value, $\theta = 1$, and the contribution of the electrochemical desorption step then becomes significant or dominant.

The gradual increase of the total current in a curving plot reflects the change in v_3 since the recombination step is the rate-determining step at this stage. This explains the experimental observations of the Tafel slope steeper than 120 mV per decade on various HER systems [22, 23] at relatively high cathodic overpotentials, as well as the chlorine electrode reaction at platinum at high anodic overpotentials [24].

Above $\eta = \sim -0.3\,\text{V}$, when $v_2 > v_3$, the electrochemical desorption path becomes more dominant and also becomes the rate-determining step resulting in the inflection of the total current curve. It is to be noted that the faster reaction characterizes the kinetics in the case of parallel reactions, as here. Above $\eta = \sim -0.4\,\text{V}$, when $k_1(1 - \theta) \approx k_2\theta$, the initial discharge step becomes rate-determining, so that the Tafel slope attains the value of $2.3RT/0.5F$.

Simulated Tafel plots for the component steps are shown in Fig. 9 for an arbitrary but rationally selected series of values of the required rate constants; it is seen that a resulting overall curve 4 can be generated that is quite similar in form to the experimental one (see Fig. 1, curve 1).

4.2. *Potential decay*

Three principal regions can be distinguished on the potential decay curves for the bright platinum electrode in 1 M KOH (Fig. 2b), especially for decay from higher initial current densities. The behaviour is then similar to the situation described for hydrogen evolution on platinum from *acidic* solutions [4]. The first region arises when $\eta > 0.09$ V, i.e. for times in the range 1 μs to ~ 0.3 ms, and corresponds [25, 26] principally to discharge of the double-layer capacitance through the non-linear faradaic reaction resistance [14]. The third region arises when $\eta < 0.06$ V, for times in the range ~ 10–160 ms and corresponds principally to the discharge of the OPD H pseudocapacitance. The second region is a relatively flat, intermediate one between the first and the third regions; it arises between 0.09 and 0.06 V, over the time range ~ 0.3–10 ms.

It is known from previous work [4] that C_ϕ is a f(η) and is only significant at low overpotentials, eventually reaching zero with increasing overpotential as θ_H reaches a kinetically controlled limiting value, < 1, or its saturation value ($\theta = 1$). Since the faradaic reaction resistance is relatively small in this case, especially for the highest initial current density referred to above, the discharge of the double-layer capacitance is near completion (when overpotentials are greater than 0.09 V) after a very short time. As the H pseudocapacitance starts to become considerable just below such a potential, it is then possible for the relatively flat intermediate region to be manifested on the potential decay curves. (In a treatment of potential decay based only on the kinetics of the consecutive steps involved, we show elsewhere [27] the significance of this arrest region in the transient.)

Since the faradaic reaction resistance becomes larger as the initial polarization current decreases (and when the initial overpotential decreases as well), the discharge time for C_{dl} (the first region) increases. Thus the regions where the discharge of C_{dl} and C_ϕ takes place overlap as shown in Figs 2 and 3.

A similar situation evidently arises in the case of the electroplated electrodes as seen in Figs 5 and 7. The second region for times in the range 0.5–10 ms is relatively flat in comparison with the two adjacent regions. This is more explicitly manifested in the derivative plots (Figs 6, 8).

4.3. *OPD H pseudocapacitance and coverage*

The pseudocapacitance behaviour of adsorbed ODP H species, evaluated from $C = i(\eta)/(-\mathrm{d}\eta\ \mathrm{d}t)$ using the current–overpotential relationship (Fig. 1) together with the differentiated potential decay curves (Fig. 3) for the bright platinum electrode in KOH, are shown in Fig. 11. The dependence of the potential decay curve on i in is expressed in the shape of the pseudocapacitance curve. For increasing values of i_{in}, the peak pseudocapacitance moves from ~ 0.02 V to ~ 0.04 V and the decline in C_ϕ becomes steeper.

Figs 12 and 13 show the C versus η plots for electroplated leaded and unleaded electrodes, respectively. Notice the much higher H capacitance involved, especially for the unleaded electrode. This is reflected by the longer times needed for the potential to decay to its reversible value (cf. Figs 2, 4, 5). On the other hand, for the bright platinum electrode in acidic solution, the pseudocapacitance is also very high (Fig. 14), corresponding to ~ 5.4 apparent equivalent monolayers of OPD H (Table 1), although the potential decay time is short, as for the bright electrode in alkaline solution. The very high C_ϕ is a result of the different value of the rate constant involved in this solution compared with that for alkali, as expressed by the different Tafel curve observed (Fig. 1), as has already been pointed out in a previous publication [4]. This difference between the behaviour in the two solutions indicates that a different H adsorption situation is involved for the two types of solution, depending on pH and thus the rate-determining step and reaction pathway involved.

Integration of the capacitance curve enables the difference of the charge transferred ($\Delta Q = \int C\,\mathrm{d}\eta$) over the potential range of the decay curve, to be evaluated, as shown in Fig. 15 for

the four different systems studied. The shapes of the curves for the three systems in alkaline solution are similar, apart from the total final difference of charge passed. The shape for the acidic solution is, however, rather different indicating again that a different state and quantity of adsorbed and absorbed H species is involved. By assuming that the H deposition charge for a monolayer on platinum is $q = 0.21\,\mathrm{mC\,cm^{-2}}$, the apparent OPD coverages of H on platinum in equivalent monolayers of H, generated under conditions of highest cathodic current densities (corresponding overpotentials can be read from Fig. 15), can be evaluated as shown in Table 1.

The apparent H coverages per real cm^2 for the bright electrode systems are similar to the results obtained previously [4], i.e. apparent multilayers are indicated (see below). Note the striking effect of the roughness factor on the apparent coverage in alkaline solutions. The 'coverages' referred to here, of course, really represent *changes* of H coverage beyond whatever value obtains at zero overpotential.

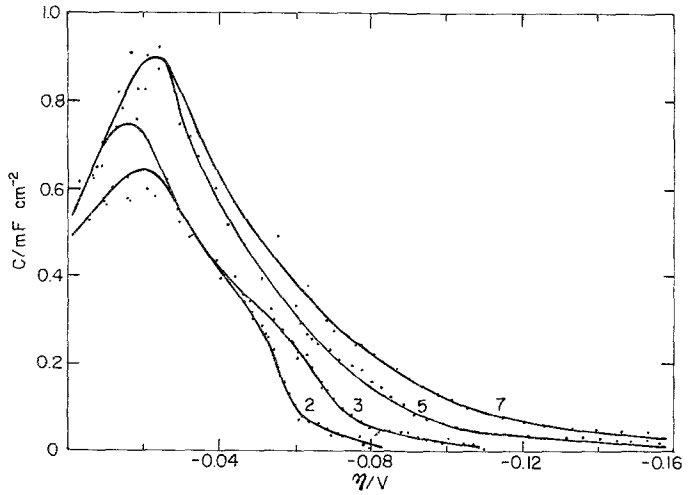

Fig. 11. Capacitance plots for bright platinum in 1 M KOH. Values of i_{in} as in Fig. 2.

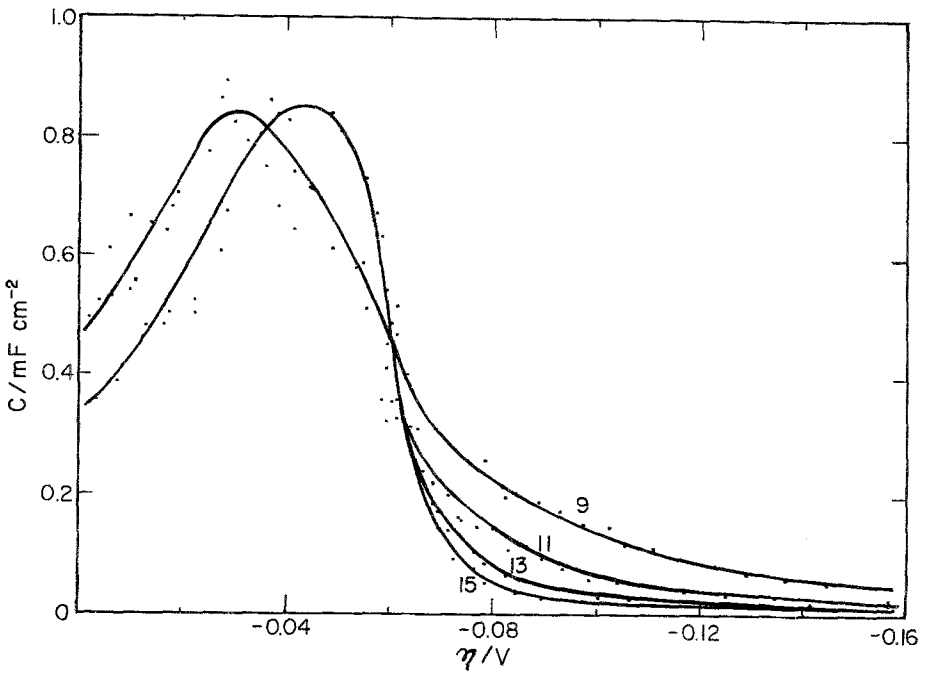

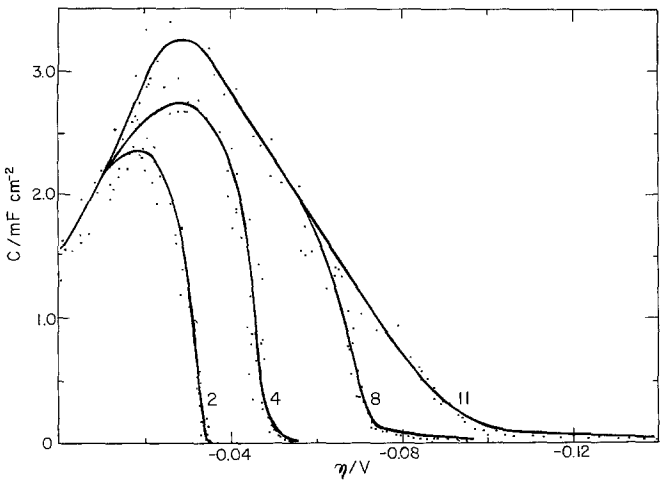

Fig. 12. Capacitance plots for leaded electrodeposited platinum in 1 M KOH. Values of i_{in} as in Fig. 5.

High apparent charges for OPD H adsorption could arise from cathodically generated H_2 present in a supersaturated boundary layer on the solution side of active platinum electrode surfaces, as supposed by Breiter [6] and adduced by him as the origin of the 2.3 $RT/2F$ Tafel slope observed at active platinum H_2 cathodes at low overpotentials. In our present and recently published [4] work on platinum, rotated electrodes were used (rotation rates > 3600 r.p.m. or here 4900 r.p.m.) in order to eliminate the possibility of anomalous results arising from local H_2 supersaturation at the electrode interface. High apparent H coverages were still indicated and hence do not seem to be an artefact due to the supersaturation effection involving H_2 but probably arise rather from some state of surface hydride formation. The latter possibility is consistent with the observation of Gileadi *et al.* [28] that cathodically generated H can diffuse into platinum.

Since it is difficult to cover an electrode with a film of H much more than one monolayer in extent, the possibility of explaining this behaviour, already suggested [4], is that in acidic solution there is formation of a hydride or 'dermasorbed' hydrogen [29, 30] phase in a relatively few atomic layers of platinum, *just in and below the surface layer*. The presence of this electroactive surface hydride phase may provide the explanation for the specially favourable electrocatalytic activity of platinum for the HER in acid solution. Although the apparent coverage in acid solution is > 1, it reaches a sharp limit with increasing overpotential, unlike the behaviour in the alkaline solution (Fig. 15), indicating the possibility of direct injection of a proton from H_3O^+ into the lattice rather than discharge of an H atom in a neutral state [4, 31] with subsequent sorption.

The half width of the pseudocapacitance peak (Figs 11–14) is narrower than that required for Langmuir adsorption [32, 33], indicating a negative g factor in the Frumkin isotherm [17, 34], i.e. some attractive interactions could be involved, greater for the acidic solution (half width =

Table 1. Numbers of apparent equivalent monolayers of OPD H at various platinum electrodes (evaluated from data from the highest initial current densities)

System	*Solution*	*Roughness factor*	*No. of equivalent monolayers (calculated on basis of real surface area)*
Bright Pt	KOH	1.8	0.30
Plated Pt, leaded	KOH	100	0.87
Plated Pt, unleaded	KOH	20	6.6
Bright Pt	H_2SO_4	1.6	5.4

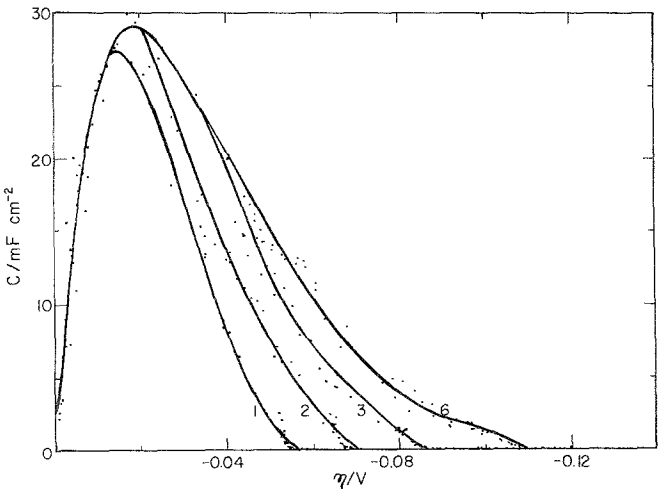

Fig. 13. Capacitance plots for unleaded electrodeposited platinum in 1 M KOH. Values of i(in) as in Fig. 7.

~ 30 mV) than for the alkaline solution (half width = ~ 50–60 mV). It is interesting to note that, for the alkaline solution, the half width is narrower as the pseudocapacitance peak (and the coverage) is higher; it is ~ 60 mV for the bright electrode, ~ 50 mV for the leaded one and ~ 45 mV for the unleaded electrode.

The formation of platinum by electrodeposition causes a dramatic increase in the apparent OPD H coverage per real cm^{-2} (based on separate UPD measurements of real area for H accommodation). The method of preparation of the electrodeposited electrode may introduce a hydride phase through co-deposition of H during the plating, similar to the situation with electrodeposited nickel–molybdenum alloys [3, 35] or in the activation of Raney nickel [35, 36]. A micro-cavity structure of such electrodes could possibly result in diffusion of H into the bulk that is later

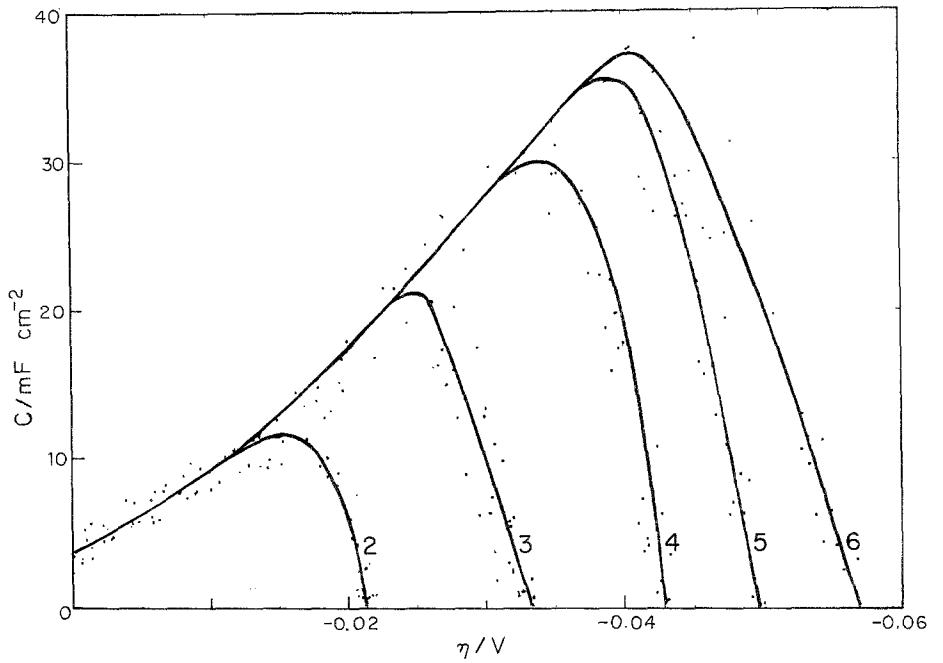

Fig. 14. Capacitance plots for bright platinum in 0.5 M H_2SO_4. i(in) values as in Fig. 4.

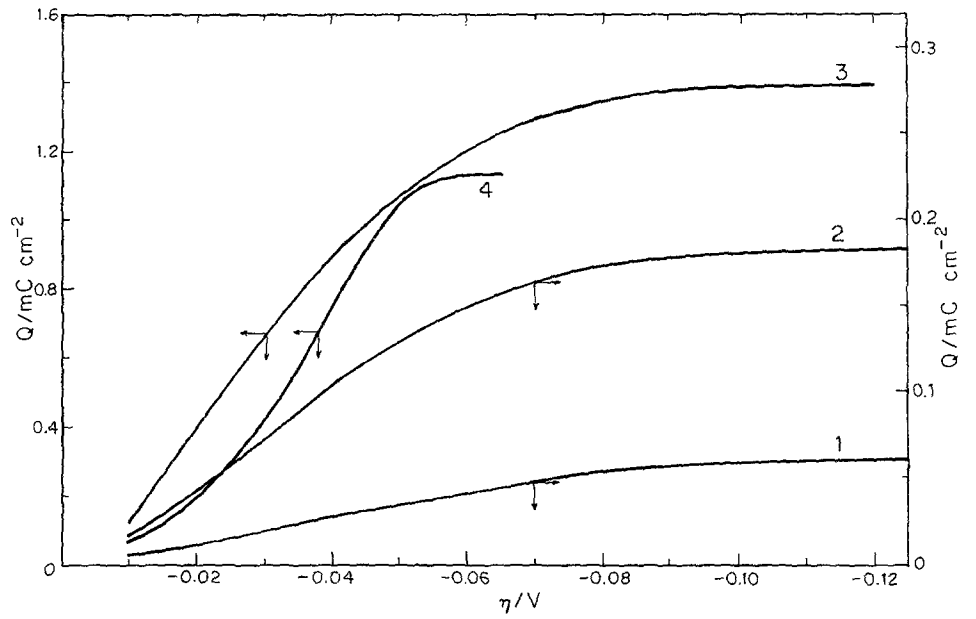

Fig. 15. The charge ΔQ transferred during the potential decay for the four systems studied: (1) bright platinum, 1 M KOH; (2) leaded electrodeposited platinum, 1 M KOH; (3) unleaded electrodeposited platinum, 1 M KOH; (4) bright platinum, 0.5 M H_2SO_4.

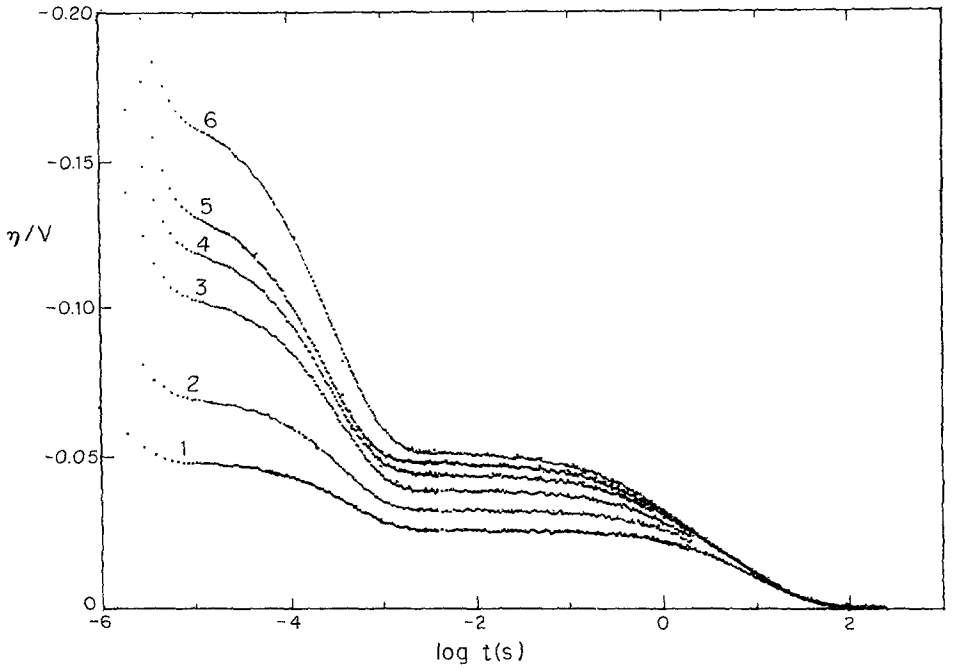

Fig. 16. Potential decay plots for the HER at a rotation rate of 4900 r.p.m. for a palladized electrode in 1 M KOH. The initial polarization currents in A cm^{-2}: (1) 0.00083; (2) 0.0017; (3) 0.0033; (4) 0.0050; (5) 0.0070; (6) 0.0083.

manifested (through its subsequent desorption) in a relatively long potential decay, i.e. more than 60 s (Fig. 7), as compared to 0.1–0.2 s for bright platinum electrodes (Figs 2, 4). The adsorption of hydrogen on such an electrode is different from that on bright platinum in acidic solution, although a formal coverage of more than unity is attained in both cases. The apparently 'dermasorbed' hydrogen in the latter electrode desorbs relatively fast during the potential decay, as is also manifested in the form of the sharp increase of the coverage with overpotential (the S-shaped curve 4 in Fig. 15), whereas for the electrodeposited platinum electrode in alkaline solution, the diffusion of the adsorbed hydrogen from the inner surfaces of the bulk of the porous electrode is a relatively long process. On comparing the potential decay curves, different shapes may be distinguished (Figs 5, 6, 7).

For the electrodeposited electrodes, a potential arrest can be seen that is similar in shape to the arrest that arises during potential decay associated with absorbed hydrogen in a thin layer of palladium electrodeposited on a platinum rotating disc electrode [23] (Fig. 16). For this case, it is well known that H sorption *into* the palladium lattice can occur. This result therefore provides support for the possible participation of bulk-type hydrogen sorption (i.e. probably H absorption) at the electrodeposited platinum electrode in its 'near-surface' region.

The behaviour of both types of electroplated platinum electrodes is quite the same apart from the total apparent H coverage attained (Table 1). The coverage for the leaded electrode is almost thrice that for the bright one, but is still much less than for the unleaded electrodeposited electrode even though the roughness factor for the latter is much smaller. These results show that, though a leaded platinum electrode preparation can be used successfully as an excellent and stable hydrogen reference electrodes [37], the presence of a minute amount of lead in the electrodeposit poisons the electrode; this effect is manifested as a substantial decrease in the OPD H coverage in steady-state H_2 evolution in comparison to that for an unleaded electrode when H_2 evolution at appreciable or significant net cathodic currents is involved. Such a result is not unexpected.

References

[1] D. M. Kolb, in 'Advances in Electrochemistry and Electrochemical Engineering', Vol. II (edited by C. Tobias and H. Gerischer), Wiley-Interscience, New York (1978) p. 125.
[2] H. Angerstein-Kozlowska and B. E. Conway, *J. Electroanal. Chem.* **95** (1979) 1.
[3] B. E. Conway and L. Bai, *J. Chem. Soc., Faraday Trans. I* **81** (1985) 1841.
[4] *Idem, J. Electroanal. Chem.* **82** (1986) 149.
[5] M. W. Breiter, C. A. Knorr and W. Volke, *Z. Elektrochem.* **59** (1955) 681.
[6] M. W. Breiter, H. Krammermeier and C. A. Knorr, *ibid.* **60** (1956) 32, 119.
[7] J. H. Ellis, *J. Amer. Chem. Soc.* **38** (1916) 737.
[8] B. E. Conway, H. Angerstein-Kozlowska, W. B. A. Sharp and E. Criddle, *Anal. Chem.* **45** (1973) 1331.
[9] E. Gileadi, E. Kirowa-Eisner and J. Penciner, in 'Interfacial Electrochemistry–An Experimental Approach', Addison-Wesley, Reading, Ma (1975) pp. 216–217.
[10] *Idem, ibid.*, p. 312.
[11] F. G. Will and C. A. Knorr, *Z. Elektrochem.* **64** (1960) 258.
[12] A. Reger, E. Peled and E. Gileadi, *J. Electrochem. Soc.* **123** (1976) 638.
[13] B. E. Conway, L. Bai and D. F. Tessier, *J. Electroanal. Chem.* **161** (1984) 39.
[14] B. V. Tilak and B. E. Conway, *Electrochim. Acta* **21** (1976) 745.
[15] B. E. Conway and P. L. Bourgault, *Trans. Faraday Soc.* **58** (1962) 593.
[16] H. B. Morley and F. E. W. Wetmore, *Can. J. Chem.* **34** (1956) 359.
[17] E. Gileadi and B. E. Conway, in 'Modern Aspects of Electrochemistry', Vol. III, (edited by J. O'M. Bockris and B. E. Conway), Butterworths, London (1964) chap. 5.
[18] A. N. Frumkin, in 'Advances in Electrochemistry and Electrochemical Engineering', Vol. 1, chap. 1, p. 65 (1961) and Vol. 3, chap. 2, p. 287 (1963), (edited by P. Delahay), Wiley-Interscience, New York.
[19] J. O'M. Bockris (ed), 'Modern Aspects of Electrochemistry', Vol. I, Butterworths, London (1954) chap. 4.
[20] M. A. V. Devanathan and S. Selvaratnam, *Trans. Faraday Soc.* **56** (1960) 1820.
[21] B. V. Tilak, C. G. Rader and B. E. Conway, *Electrochim. Acta* **22** (1977) 1167.
[22] M. Enyo and T. Maoka, *J. Electroanal. Chem.* **108** (1980) 277.
[23] M. Elam and B E. Conway, *J. Electrochem. Soc..*, in press.
[24] T. Yokoyama and M. Enyo, *Electrochim. Acta* **15** (1970) 1921.
[25] M. W. Breiter, *J. Electroanal. Chem.* **14** (1967) 407.

[26] J. A. V. Butler and J. F. Armstrong, *Trans. Faraday Soc.* **29** (1933) 1261.
[27] D. A. Harrington and B. E. Conway, *J. Electroanal. Chem.* **221** (1987) 1.
[28] E. Gileadi, M. A. Fullenwider and J. O'M. Bockris, *J. Electrochem. Soc.* **113** (1965) 976.
[29] S. Schuldiner and T. B. Warner, *J. Electrochem. Soc.* **112** (1965) 212.
[30] *Idem, Electrochim. Acta* **11** (1966) 307.
[31] W. Palczewska, *Bull. Acad. Polon., Ser. Sci. Chim.* **12** (1964) 817.
[32] B. E. Conway and E. Gileadi, *Electrochim. Acta* **11** (1966) 321.
[33] H. Angerstein-Kozlowska, J. Klinger and B. E. Conway, *J. Electroanal. Chem.* **75** (1977) 45.
[34] B. E. Conway, E. Gileadi and M. Dzieciuch, *Electrochim. Acta* **8** (1963) 143.
[35] B. E. Conway, H. Angerstein-Kozlowska, M. A. Sattar and B. V. Tilak, *J. Electrochem. Soc.* **130** (1983) 1825.
[36] H. H. Ewe, *Electrochim. Acta* **17** (1972) 2267.
[37] D. I. G. Ives and G. J. Janz, 'Reference Electrodes, Theory and Practice', Academic Press, New York (1961) p. 107.